Colloidal Dynamics on a Choreographic Time Crystal

András Libál,[1,2] Tünde Balázs,[2] C. Reichhardt,[1] and C. J. O. Reichhardt[1]
[1]Theoretical Division and Center for Nonlinear Studies, Los Alamos National Laboratory, Los Alamos, New Mexico 87545, USA
[2]Mathematics and Computer Science Department, Babeş-Bolyai University, Cluj 400084, Romania

(Received 10 December 2019; revised manuscript received 17 March 2020; accepted 4 May 2020; published 21 May 2020)

A choreographic time crystal is a dynamic lattice structure in which the points comprising the lattice move in a coordinated fashion. These structures were initially proposed for understanding the motion of synchronized satellite swarms. Using simulations, we examine colloids interacting with a choreographic crystal consisting of traps that could be created optically. As a function of the trap strength, speed, and colloidal filling fraction, we identify a series of phases including states where the colloids organize into a dynamic chiral loop lattice as well as a frustrated induced liquid state and a choreographic lattice state. We show that transitions between these states can be understood in terms of vertex frustration effects that occur during a certain portion of the choreographic cycle. Our results can be generalized to a broader class of systems of particles coupled to choreographic structures, such as vortices, ions, cold atoms, and soft matter systems.

DOI: 10.1103/PhysRevLett.124.208004

Crystalline states arise throughout nature and are characterized by their symmetries. Since these structures are static in time, they can be described by a single snapshot. Recently, there have been proposals for dynamic crystals containing points that move in a synchronized fashion such that a single time snapshot does not reveal all the symmetries in the system. These structures are called choreographic crystals [1], and they are composed of a collection of points that undergo a series of repeated moves to form varying patterns that recur over time. In some such systems, the ground states themselves are also periodic in time, forming what are called time crystals [2,3]. Generally, time crystal systems must be driven out of equilibrium and contain some form of dissipation, so they are not in a true ground state. Nevertheless, there is growing interest in creating and studying the properties of classical [2–6] and quantum [7–9] time and choreographic crystals in condensed matter, atomic, and even cosmological systems [10,11]. Choreographic crystals represent a new type of structure, and there are many open questions, including how to realize these states, what their properties are, and whether they could be coupled to other systems.

Here, we examine a system of dynamic traps that form a choreographic crystal coupled to an assembly of colloidal particles. There have been many studies of colloidal trapping on static crystalline substrates [12–19] or quasiperiodic lattices [20,21], showing melting and commensurate-incommensurate transitions. Studies of the dynamics of colloids driven over such crystalline substrates reveal locking of the colloid motion to a substrate lattice symmetry direction [22–26], depinning of incommensurate kinks and antikinks [27–30], and a diverse array of other dynamical phenomena [31,32]. Individual traps can be dynamically controlled and moved [33] or flashed on and off [34,35], so with appropriate rules for translation, it should be feasible to create a choreographic lattice of optical traps that couple to colloidal particles. Beyond colloids, optical trapping lattices have been created for cold atom systems [36,37], ions [38], vortices in Bose-Einstein condensates [39], and vortices in type-II superconductors [40], so similar choreographic lattices could be created for these systems. Choreographic trap arrays thus represent a new type of lattice for studies of commensuration effects and dynamics.

In our simulations, we find three generic phases of colloid dynamics depending on the strength and speed of the traps as well as the filling fraction or ratio of the number of colloids to the number of traps. In the weakly coupled regime, the colloids are temporarily trapped and organize into a dynamical chiral loop crystal. In the partially coupled regime, where a given colloid is dragged by a trap for a varied length of time before decoupling from the trap, a liquidlike state appears. In the strong coupling regime, the colloids are permanently locked to the traps and themselves form a choreographic crystal. At higher filling fractions, we observe phases in which traps containing multiple colloids interact with interstitial colloids in the regions between traps, while at high trap velocities, the colloids decouple from the traps. We map out a dynamic phase diagram as a function of the trap strength and velocity. We also show that the transition into and out of the liquid phase is the result of a vertex frustration effect, similar to that found in triangular artificial spin ice [41–43], which appears during the portion of the choreographic cycle when the trap spacing reaches its minimum value.

Simulation.—We conduct simulations of pointlike colloidal particles in a two-dimensional box of size

$L \times L\sqrt{3}/2$ with $L = 96.0$ and periodic boundary conditions. The sample contains $N_{\rm trap} = 576$ trapping sites of radius $R_{\rm trap} = 1.0$ which are initially arranged in a 24×24 hexagonal lattice with lattice constant $a = 4.0$, large enough to ensure that traps never overlap when they are translated. To create the choreographic crystal, we use the rules for motion introduced in Ref. [1]. The traps are divided into three subsets $\alpha_{1,2,3}$, as shown schematically in Fig. 1(a). Each subset moves in a direction given by the vector (x, y), which has the value $(-0.5, -\sqrt{3}/2)$ for α_1, (1,0) for α_2 and $(-0.5, +\sqrt{3}/2)$ for α_3. The traps are initialized in a hexagonal lattice, as shown in Fig. 1(a), and each trap moves in a straight line with a velocity $v_{\rm trap}$. The original hexagonal ordering is restored after every τ time units, where $\tau = a/(v_{\rm trap}\Delta t)$ and Δt is the size of a simulation time step. In Fig. 1(b), we illustrate the portion of the cycle in which the spacing between the traps reaches its smallest value.

The sample contains N_c colloidal particles, and we characterize the filling fraction as $f = N_c/N_{\rm trap}$. The dynamical evolution of the colloids is given by the following overdamped equation of motion:

$$\frac{1}{\eta}\frac{\Delta \mathbf{r}_i}{\Delta t} = \mathbf{F}^i_{pp} + \mathbf{F}^i_{\rm trap}, \tag{1}$$

where $\eta = 1$ is the viscosity. The interaction potential between two charged colloidal particles i and j at a distance of $\mathbf{r}_{ij}$ is given by a screened Coulomb interaction: $\mathbf{F}^{ij}_{pp} = \exp(-r/r_0)\hat{\mathbf{r}}_{ij}/r^2$, where $r_0 = 4.0$ is the screening length. The interaction between colloid i and trap k is given by a simple finite-range harmonic spring: $\mathbf{F}_{\rm trap} = (F_{\rm trap} r_{ik}/R_{\rm trap})\hat{\mathbf{r}}_{ik}$, where $F_{\rm trap}$ is the maximum force at the edge of the trap and r_{ik} is the distance between the colloid and the center of the trap. Our dimensionless unit of length is r_0/a, and our dimensionless timescale is $\tau = 1/\eta$, where we take $\eta = 1.0$. The colloids are initialized at random locations with a specified minimum possible spacing between adjacent colloids. The traps are then set into motion, and the system eventually settles into a steady state.

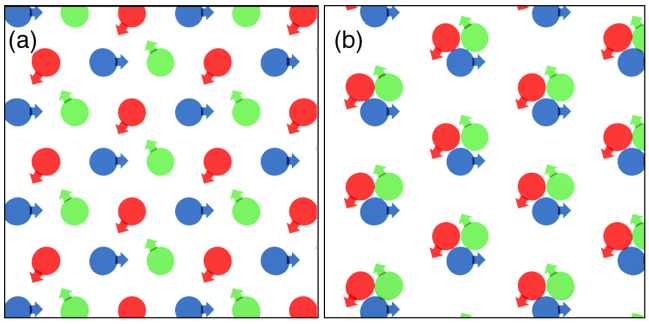

FIG. 1. (a) Schematic of a choreographic lattice composed of three subsets of traps $\alpha_{1,2,3}$ that move at a velocity $v_{\rm trap}$ in a synchronized manner according to the rules given in Ref. [1]. Each subset of traps moves in a different direction defined by the vector (x, y) which has the value $(-0.5, -\sqrt{3}/2)$ for α_1 (red), (1,0) for α_2 (blue), and $(-0.5, +\sqrt{3}/2)$ for α_3 (green), as indicated by the arrows. The traps never overlap, and they reform the original triangular lattice ordering shown in (a) every τ time units. (b) Image of the trap positions at the point in the cycle where the spacing between traps reaches its smallest value.

Results.—We first consider the weak coupling regime with $F_{\rm trap} = 0.4$ and $v_{\rm trap} = 0.5$ at a filling of $f = 1.0$, where individual colloids can be trapped for a short time but move a distance less than a trap lattice constant. In Fig. 2(a), we illustrate the colloid and trap locations at the beginning of the simulation when the colloid positions are disordered. After several cycles of trap motion, the colloids organize into the crystalline state shown in Fig. 2(b), where the diffusion drops to zero and the colloids move in a nonoverlapping pattern of counterclockwise triangular loops, a state that we term a dynamic chiral lattice (DCL). The size of the colloidal orbits decreases with decreasing trap strength and falls to zero when $F_{\rm trap} = 0$, where the colloids form a static hexagonal lattice. At $F_{\rm trap} = 0.7$, shown in Fig. 2(c), each trap permanently captures one colloid [44]. The image of the trajectories of some of the colloids in Fig. 2(d) indicates that each colloid follows a straight line path. Here, the traps are strong enough to overcame the colloid-colloid repulsive force even when the traps reach their point of closest approach, so the colloids themselves form a choreographic lattice (ChL). Although there is no net drift motion averaged over all of the colloids, individual colloids undergo ballistic motion, so that the mean squared displacement $d(t) = N_c^{-1}\sum_i^{N_c} |\mathbf{r}_i(t) - \mathbf{r}_i(t_0)|^2$ obeys $d(t) \propto t^2$ in the ChL phase. When $F_{\rm trap}$ is increased further, we observe the same structure and dynamics.

At intermediate trapping strengths between the DCL and ChL states, the system forms a partially coupled or disordered state in which each colloid is dragged by a trap over a distance of several lattice constants before it becomes dislodged. We show a snapshot of this state in Fig. 2(e) for $F_{\rm trap} = 0.54$, where the colloidal positions are disordered in the steady state. The corresponding trajectories of some of the colloids in Fig. 2(f) show that there is short-time ballistic behavior when the colloids are dragged; however, the longer-time behavior is diffusive with $d(t) \propto t$.

The transition between the DCL and the ChL states can be understood by considering the portion of the cycle in which the traps are closest together, shown in Fig. 1(b). We can think of this structure in terms of a vertex picture similar to that found in triangular colloidal spin ice systems [41–43]. An occupied trap is the equivalent of a particle close to the vertex. When vertex states are labeled by the total number of particles that are close to the vertex (0-, 1-, 2-, or 3-in), the ice-rule-obeying state contains 1- and 2-in vertices. In Fig. 3, we illustrate the trap and colloid positions at the point of closest approach along with the corresponding triangular colloidal spin ice vertex state.

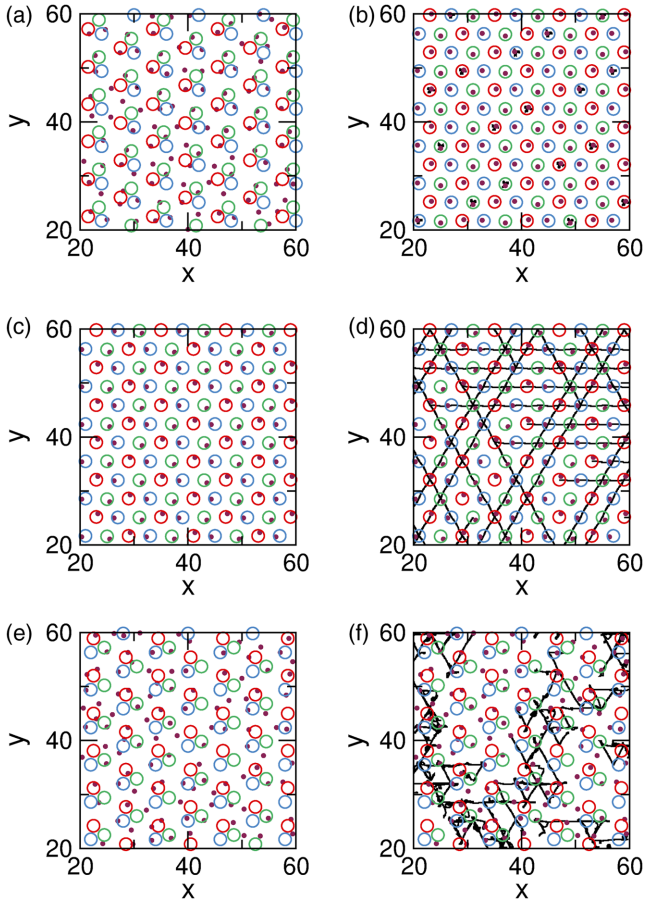

FIG. 2. Trap positions (open circles) and colloid positions (dots) in a portion of the sample at $v_{\mathrm{trap}} = 0.5$ for a filling of $N_c/N_{\mathrm{trap}} = 1.0$. Black lines in (b), (d), and (e) are the trajectories of a subset of the colloids. (a) The weak coupling regime at $F_{\mathrm{trap}} = 0.4$ in the initial disordered state. (b) The same system after it has organized to a crystalline state. Each colloid executes a small counterclockwise triangular loop, forming a DCL. (c) $F_{\mathrm{trap}} = 0.7$, where each trap permanently captures one colloid. As shown in (d), the colloids now move in straight lines and form a ChL. (e) The frustrated liquid state at $F_{\mathrm{trap}} = 0.54$, where the system disorders and colloids can be dragged various distances as a function of time, as indicated by the trajectories shown in (f). Videos illustrating the dynamics of these phases are available in Supplemental Material [44].

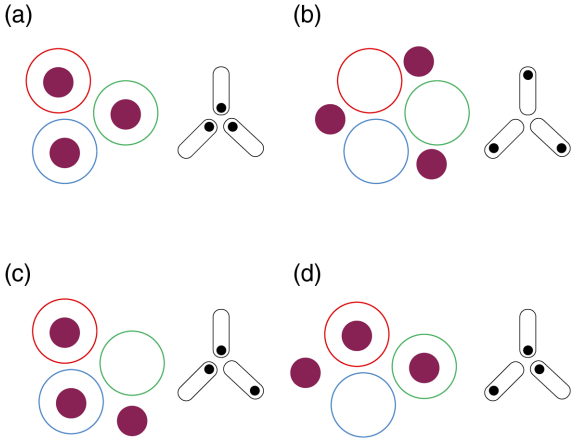

FIG. 3. Schematics (left) of the vertex states at the point of closest approach of the traps along with schematics (right) of the matching artificial spin ice vertex state. (a) For large F_{trap}, the colloids remain inside the traps, 3-in vertices are stable, and the ChL state appears. (b) For small F_{trap}, all of the colloids escape from the traps, 0-in vertices are stable, and the DCL state appears. (c),(d) For intermediate F_{trap}, 2-in vertex states are stable; however, there are three equivalent ways to form a 2-in state, two of which are illustrated in (c) and (d). As a result, the system is frustrated and becomes disordered.

When all three traps are occupied, as in Fig. 3(a), the resulting 3-in state is the highest-energy configuration due to the repulsive colloid-colloid interactions, while if all three traps are empty, as in Fig. 3(b), the corresponding vertex is in the lowest-energy 0-in state. For large F_{trap}, the trapping energy overwhelms the colloid-colloid interactions, stabilizing the 3-in vertex state and producing the ChL phase with ordered dynamics. For small F_{trap}, the colloidal interaction energy dominates and stabilizes the 0-in vertex state, producing the ordered DCL state. At intermediate F_{trap}, 1- and 2-in vertices are favored, where the 2-in vertex has higher energy, and the system is highly degenerate similar to the triangular colloidal spin ice. There is only one possible arrangement of a system full of 3- or 0-in vertices, but many possible arrangements of a system full of 1- and 2-in vertices. For example, two distinct 2-in vertex configurations appear in Figs. 3(c) and 3(d). The resulting frustration at intermediate trap strength prevents the colloids from reaching a repeatable ordered state, since, each time the traps reach their point of closest approach, a different energy-equivalent ice-rule-obeying colloid configuration can appear, giving a disordered structure. For longer-range interactions spanning a distance of multiple vertices, the ice degeneracy could be lifted, causing new types of time-repeated dynamical states to occur. Other types of choreographic crystals might not have the same frustration effects during any portion of the cycle or might exhibit choreographic crystals that are frustrated during the entire cycle.

Transitions between the states can occur with changing the trap speed or strength, since the coupling between the colloids and the traps weakens when v_{trap} increases. To characterize this, in Fig. 4(a), we plot $\langle v_c \rangle / v_{\mathrm{trap}} = N_c^{-1} \sum_i^{N_c} |\mathbf{v}_i| / v_{\mathrm{trap}}$ for the system in Fig. 2. If $\langle v_c \rangle / v_{\mathrm{trap}} = 1.0$, all the colloids are trapped and match the trap velocity in the ChL state. For $\langle v_c \rangle / v_{\mathrm{trap}} < 0.3$, the colloids are only temporarily trapped and the DCL state appears, while for $0.3 < \langle v_c \rangle / v_{\mathrm{trap}} < 0.9$, the system is in the disordered state. A plateau near $\langle v_c \rangle / v_{\mathrm{trap}} = 0.33$ corresponds to a prevalence of 1-in states with 1/3 of the traps occupied. Even in the DCL state, $\langle v_c \rangle / v_{\mathrm{trap}} > 0$, since the traps are occupied for at least a short period of

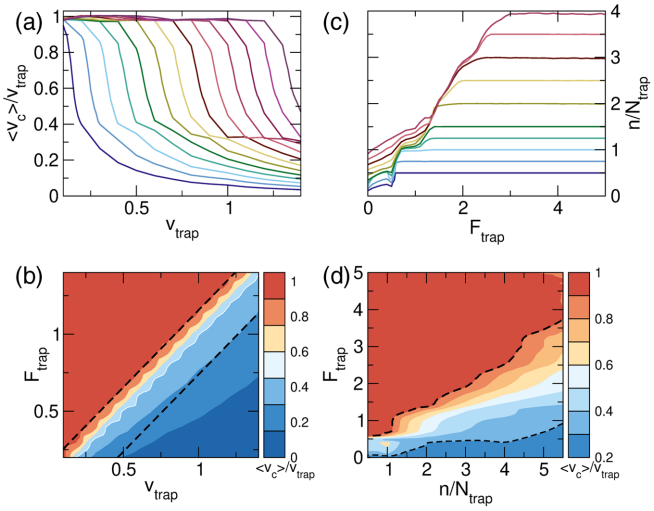

FIG. 4. (a) $\langle v_c \rangle / v_{\mathrm{trap}}$ versus v_{trap} for the system in Fig. 2 with $f = 1$ and $F_{\mathrm{trap}} = 0.2$, 0.3, 0.4, 0.5, 0.6, 0.7, 0.8, 0.9, 1.0, 1.1, 1.2, 1.3, and 1.4, from bottom to top. The ChL phase appears when $\langle v_c \rangle / v_{\mathrm{trap}} = 1.0$, the DCL phase has $\langle v_c \rangle / v_{\mathrm{trap}} < 1/3$, and outside these ranges is the frustrated liquid state. (b) Dynamic phase diagram as a function of F_{trap} versus v_{trap}. Dashed lines are theoretical estimates for the boundaries between the ChL, DCL, and intermediate frustrated liquid states. (c) The average number n/N_{trap} of colloids in each trap versus F_{trap} for $v_{\mathrm{trap}} = 0.5$ and filling fractions of $f = 0.5$, 0.75, 1.0, 1.25, 1.5, 2.0, 2.5, 3.0, 3.5, and 4.0, from bottom to top. (d) Dynamic phase diagram as a function of F_{trap} versus n/N_{trap}. Dashed lines indicate boundaries between the ChL, DCL, and intermediate frustrated liquid states.

time. As F_{trap} increases, the onset of the ChL phase shifts to lower values of v_{trap}.

In Fig. 4(b), we plot a dynamic phase diagram as a function of F_{trap} versus v_{trap} for the system in Fig. 4(a), indicating the regions where the DCL, ChL, and disordered phases occur. The boundaries in Fig. 4(b) can be understood by considering the nearest-neighbor forces at the distance of closest approach $R_c = 2$. In the ChL phase, all of the particles must remain trapped at closest approach, which occurs when $F_{\mathrm{trap}} \geq \eta v_{\mathrm{trap}} + F_{pp}(R_c)$. The ChL phase should occur for $F_p > 1.1516$ when $v_{\mathrm{trap}} = 1.0$, in agreement with Fig. 4(b). In the DCL state, all the particles must be out of the traps at closest approach, which occurs when $F_{\mathrm{trap}} \leq \eta v_{\mathrm{trap}} - 2\sin(60°) F_{pp}(R_c)$. For $v_{\mathrm{trap}} = 1.0$, the DCL phase should appear when $F_{\mathrm{trap}} \leq 0.737$, in agreement with the figure.

For changing filling f, we find the same general features described above when $f \leq 1$, while interstitial colloids appear when $f > 1$. For a sufficiently large trap strength, all the colloids are eventually trapped, and the ChL phase appears with clusters of n/N_{trap} colloids at each trap, where n is the time-averaged number of trapped colloids. When the traps are too weak to capture f colloids apiece, more complex states appear where multiply occupied traps coexist with interstitial colloids. As f increases, the disordered phase grows in extent. In Fig. 4(c), we plot n/N_{trap} versus F_{trap} for varied filling. A series of plateaus occur at $n/N_{\mathrm{trap}} = 1/f$ for large F_{trap} when no interstitial colloids are present. Jumps in n/N_{trap} occur when multiple trap occupancy and commensuration effects overlap. For example, at $n/N_{\mathrm{trap}} = 0.5$, 1.0, and 1.5, commensurate ordered states appear, while the higher-order steps near $n/N_{\mathrm{trap}} = 2.5$, 3.0, and 4.0 correspond to partially ordered states at higher fillings. Additional ordering near integer and rational f was observed in systems with static pinning such as vortices in type-II superconductors [45–47]. In Fig. 4(d), we plot a dynamic phase diagram as a function of F_{trap} versus n/N_{trap}, highlighting the strongly coupled regime or ChL phase, the weakly coupled DCL regime, and the intermediate regime consisting of disordered states in which multiply trapped colloids can coexist with interstitial colloids.

We consider a fixed colloid-colloid interaction strength and range where nearest-neighbor interactions dominate, as in most experiments. If longer-range interactions become important, the disordered phase could grow in extent, but additional long-range ordered phases could also arise. Experimentally, this system could be realized with time-dependent [35], moving [48–50], rastered [51], or dynamically manipulated [52,53] optical traps. To achieve artificial periodic boundary conditions, a trap that reaches the sample edge would be shut off and replaced by a trap on the other side of the sample, with colloid capture and release occurring in a bath area surrounding the sample. Alternatively, traps could be driven back and forth periodically through the sample.

Summary.—We have examined a choreographic lattice of traps that move in a synchronized fashion without overlap. When the traps are coupled to an assembly of colloidal particles with repulsive screened Coulomb interaction, we observe several different dynamical regimes: a dynamically ordered chiral crystal state in which the colloids are temporarily trapped, follow loop orbits, and have zero net diffusion; a strongly coupled state in which the colloids themselves form a choreographic lattice with ballistic motion; and an intermediate frustrated liquid state with long-time diffusive behavior. The different states can be understood by mapping the closest approach of the traps to triangular colloidal spin ice vertices. At intermediate coupling, multiple vertex states with equivalent energies are possible, producing frustration and a disordered configuration similar to that found in triangular colloidal spin ice. Our results could be generalized to a wide variety of choreographic time crystals with dynamical substrates and represent a new particle assembly-periodic substrate system in which commensuration effects, dynamic phases, and melting can be explored using optical traps or other methods to create a translating trap array. Similar results should appear for vortices, cold atoms, and ions coupled to a choreographic lattice.

This work was supported by the U.S. Department of Energy through the Los Alamos National Laboratory. Los Alamos National Laboratory is operated by Triad National Security, LLC, for the National Nuclear Security Administration of the U.S. Department of Energy (Contract No. 892333218NCA000001).

[1] L. Boyle, J. Y. Khoo, and K. Smith, Symmetric Satellite Swarms and Choreographic Crystals, Phys. Rev. Lett. **116**, 015503 (2016).
[2] A. Shapere and F. Wilczek, Classical Time Crystals, Phys. Rev. Lett. **109**, 160402 (2012).
[3] K. Sacha and J. Zakrzewski, Time crystals: A review, Rep. Prog. Phys. **81**, 016401 (2018).
[4] F. Flicker, Time quasilattices in dissipative dynamical systems, SciPost Phys. **5**, 001 (2018).
[5] N. Y. Yao, C. Nayak, L. Balents, and M. P. Zaletel, Classical discrete time crystals, Nat. Phys. **16**, 438 (2020).
[6] J. Dai, A. J. Niemi, X. Peng, and F. Wilczek, Truncated dynamics, ring molecules, and mechanical time crystals, Phys. Rev. A **99**, 023425 (2019).
[7] F. Wilczek, Quantum Time Crystals, Phys. Rev. Lett. **109**, 160401 (2012).
[8] T. Li, Z.-X. Gong, Z.-Q. Yin, H. T. Quan, X. Yin, P. Zhang, L.-M. Duan, and X. Zhang, Space-Time Crystals of Trapped Ions, Phys. Rev. Lett. **109**, 163001 (2012).
[9] J. Zhang, P. W. Hess, A. Kyprianidis, P. Becker, A. Lee, J. Smith, G. Pagano, I. D. Potirniche, A. C. Potter, A. Vishwanath, N. Y. Yao, and C. Monroe, Observation of a discrete time crystal, Nature (London) **543**, 217 (2017).
[10] M. Bošković, F. Duque, M. C. Ferreira, F. S. Miguel, and V. Cardoso, Motion in time-periodic backgrounds with applications to ultralight dark matter halos at galactic centers, Phys. Rev. D **98**, 024037 (2018).
[11] D. A. Easson and T. Manton, Stable cosmic time crystals, Phys. Rev. D **99**, 043507 (2019).
[12] A. Chowdhury, B. J. Ackerson, and N. A. Clark, Laser-Induced Freezing, Phys. Rev. Lett. **55**, 833 (1985).
[13] Q.-H. Wei, C. Bechinger, D. Rudhardt, and P. Leiderer, Experimental Study of Laser-Induced Melting in Two-Dimensional Colloids, Phys. Rev. Lett. **81**, 2606 (1998).
[14] P. T. Korda, G. C. Spalding, and D. G. Grier, Evolution of a colloidal critical state in an optical pinning potential landscape, Phys. Rev. B **66**, 024504 (2002).
[15] C. Reichhardt and C. J. Olson, Novel Colloidal Crystalline States on Two-Dimensional Periodic Substrates, Phys. Rev. Lett. **88**, 248301 (2002).
[16] M. Brunner and C. Bechinger, Phase Behavior of Colloidal Molecular Crystals on Triangular Light Lattices, Phys. Rev. Lett. **88**, 248302 (2002).
[17] R. Agra, F. van Wijland, and E. Trizac, Theory of Orientational Ordering in Colloidal Molecular Crystals, Phys. Rev. Lett. **93**, 018304 (2004).
[18] A. Ortiz-Ambriz and P. Tierno, Engineering of frustration in colloidal artificial ices realized on microfeatured grooved lattices, Nat. Commun. **7**, 10575 (2016).
[19] T. Brazda, A. Silva, N. Manini, A. Vanossi, R. Guerra, E. Tosatti, and C. Bechinger, Experimental Observation of the Aubry Transition in Two-Dimensional Colloidal Monolayers, Phys. Rev. X **8**, 011050 (2018).
[20] J. Mikhael, J. Roth, L. Helden, and C. Bechinger, Archimedean-like tiling on decagonal quasicrystalline surfaces, Nature (London) **454**, 501 (2008).
[21] M. Schmiedeberg and H. Stark, Colloidal Ordering on a 2D Quasicrystalline Substrate, Phys. Rev. Lett. **101**, 218302 (2008).
[22] P. T. Korda, M. B. Taylor, and D. G. Grier, Kinetically Locked-in Colloidal Transport in an Array of Optical Tweezers, Phys. Rev. Lett. **89**, 128301 (2002).
[23] M. P. MacDonald, G. C. Spalding, and K. Dholakia, Microfluidic sorting in an optical lattice, Nature (London) **426**, 421 (2003).
[24] C. Reichhardt and C. J. Olson Reichhardt, Dynamical Ordering and Directional Locking for Particles Moving Over Quasicrystalline Substrates, Phys. Rev. Lett. **106**, 060603 (2011).
[25] T. Bohlein and C. Bechinger, Experimental Observation of Directional Locking and Dynamical Ordering of Colloidal Monolayers Driven Across Quasiperiodic Substrates, Phys. Rev. Lett. **109**, 058301 (2012).
[26] X. Cao, E. Panizon, A. Vanossi, N. Manini, and C. Bechinger, Orientational and directional locking of colloidal clusters driven across periodic surfaces, Nat. Phys. **15**, 776 (2019).
[27] T. Bohlein, J. Mikhael, and C. Bechinger, Observation of kinks and antikinks in colloidal monolayers driven across ordered surfaces, Nat. Mater. **11**, 126 (2012).
[28] A. Vanossi, N. Manini, and E. Tosatti, Static and dynamic friction in sliding colloidal monolayers, Proc. Natl. Acad. Sci. U.S.A. **109**, 16429 (2012).
[29] J. Hasnain, S. Jungblut, and C. Dellago, Dynamic phases of colloidal monolayers sliding on commensurate substrates, Soft Matter **9**, 5867 (2013).
[30] D. McDermott, J. Amelang, C. J. Olson Reichhardt, and C. Reichhardt, Dynamic regimes for driven colloidal particles on a periodic substrate at commensurate and incommensurate fillings, Phys. Rev. E **88**, 062301 (2013).
[31] J. Loehr, M. Loenne, A. Ernst, D. de las Heras, and T. M. Fischer, Topological protection of multiparticle dissipative transport, Nat. Commun. **7**, 11745 (2016).
[32] P. Tierno, T. H. Johansen, and T. M. Fischer, Localized and Delocalized Motion of Colloidal Particles on a Magnetic Bubble Lattice, Phys. Rev. Lett. **99**, 038303 (2007).
[33] D. G. Grier, A revolution in optical manipulation, Nature (London) **424**, 810 (2003).
[34] A. Libál, C. Reichhardt, B. Jankó, and C. J. O. Reichhardt, Dynamics, Rectification, and Fractionation for Colloids on Flashing Substrates, Phys. Rev. Lett. **96**, 188301 (2006).
[35] T. Brazda, C. July, and C. Bechinger, Experimental observation of Shapiro-steps in colloidal monolayers driven across time-dependent substrate potentials, Soft Matter **13**, 4024 (2017).
[36] H. P. Büchler, G. Blatter, and W. Zwerger, Commensurate-Incommensurate Transition of Cold Atoms in an Optical Lattice, Phys. Rev. Lett. **90**, 130401 (2003).
[37] C. Muldoon, L. Brandt, J. Dong, D. Stuart, E. Brainis, M. Himsworth, and A. Kuhn, Control and manipulation of cold atoms in optical tweezers, New J. Phys. **14**, 073051 (2012).

[38] J. Schmidt, A. Lambrecht, P. Weckesser, M. Debatin, L. Karpa, and T. Schaetz, Optical Trapping of Ion Coulomb Crystals, Phys. Rev. X **8**, 021028 (2018).
[39] S. Tung, V. Schweikhard, and E. A. Cornell, Observation of Vortex Pinning in Bose-Einstein Condensates, Phys. Rev. Lett. **97**, 240402 (2006).
[40] I. S. Veshchunov, W. Magrini, S. V. Mironov, A. G. Godin, J. B. Trebbia, A. I. Buzdin, Ph. Tamarat, and B. Lounis, Optical manipulation of single flux quanta, Nat. Commun. **7**, 12801 (2016).
[41] A. Libál, C. Nisoli, C. J. O. Reichhardt, and C. Reichhardt, Inner Phases of Colloidal Hexagonal Spin Ice, Phys. Rev. Lett. **120**, 027204 (2018).
[42] C. Nisoli, Unexpected Phenomenology in Particle-Based Ice Absent in Magnetic Spin Ice, Phys. Rev. Lett. **120**, 167205 (2018).
[43] A. Ortiz-Ambriz, C. Nisoli, C. Reichhardt, C. J. O. Reichhardt, and P. Tierno, Ice rule and emergent frustration in particle ice and beyond, Rev. Mod. Phys. **91**, 041003 (2019).
[44] See Supplemental Material at http://link.aps.org/supplemental/10.1103/PhysRevLett.124.208004 for Supplemental movies.
[45] C. Reichhardt, C. J. Olson, and F. Nori, Commensurate and incommensurate vortex states in superconductors with periodic pinning arrays, Phys. Rev. B **57**, 7937 (1998).
[46] C. Reichhardt and N. Grønbech-Jensen, Critical currents and vortex states at fractional matching fields in superconductors with periodic pinning, Phys. Rev. B **63**, 054510 (2001).
[47] G. R. Berdiyorov, M. V. Milošević, and F. M. Peeters, Novel Commensurability Effects in Superconducting Films with Antidot Arrays, Phys. Rev. Lett. **96**, 207001 (2006).
[48] D. Babič and C. Bechinger, Noise-Enhanced Performance of Ratchet Cellular Automata, Phys. Rev. Lett. **94**, 148303 (2005).
[49] J. E. Curtis, B. A. Koss, and D. G. Grier, Dynamic holographic optical tweezers, Opt. Commun. **207**, 169 (2002).
[50] D. G. Grier and Y. Roichman, Holographic optical trapping, Appl. Opt. **45**, 880 (2006).
[51] F. A. Lavergne, H. Wendehenne, T. Baeuerle, and C. Bechinger, Group formation and cohesion of active particles with visual perception-dependent motility, Science **364**, 70 (2019).
[52] S. Ghosh and A. Ghosh, Mobile nanotweezers for active colloidal manipulation, Sci. Rob. **3**, eaaq0076 (2018).
[53] S. Ghosh and A. Ghosh, All optical dynamic nanomanipulation with active colloidal tweezers, Nat. Commun. **10**, 4191 (2019).